Acoustic absorbtion material optimisation in the mid-high frequency range

Sébastien Besset, Mohamed Ichchou

Acoustic absorbtion material optimisation in the mid-high frequency range

S. Besset and M.M. Ichchou
D2S/LTDS, École Centrale de Lyon,
36 av. Guy de Collongue,
69134 Ecully cedex, France

Applied acoustics, 72(9), 632-638, 2011

Abstract

Acoustic modelling, applicable to poroelastic materials in a wide frequency range, is time consuming. This paper offers an energy method for optimising absorption coefficients at the boundaries of an acoustic cavity. The influence of absorption coefficients on this proposed energy method will be examined first. The next step will seek to optimise the location of absorbing materials. Numerical results will prove the method's effectiveness. Improvements in the overall optimisation process will also be proposed. A model based on polynomial interpolations will be developed in order to further reduce time consumption.

keywords: Absorption coefficient; Mid-frequency range; Energy methods

1 Introduction

Acoustical insulation is a major issue in engineering applications such as transportation (aircraft, automotive industry) or civil engineering. Noise mitigation is indeed required for the sake of public comfort. The level of noise can often be reduced through absorbent materials. Poroelastic materials such as foams are among the noise treatment packets. The weight and location of such additional materials however become key concerns. The optimisation process has received considerable attention as part of this noise abatement strategy. Predictive numerical modelling serves as the basis for determining optimisation quality. Noise prediction focuses on the widest frequency band of interest. The entire audible frequency range (up to 20 kHz) should in fact be taken into account by the numerical modelling approach. Classically speaking, pressure noise displays three different types of behaviour as frequency increases (see Figure 1. The first band defines the low-frequency region, in which finite element methods and/or boundary element methods are well adapted. The second and third frequency regions

define the mid- and high-frequency domains. In the open literature, many optimisation processes are based on finite element or boundary element methods, and only very few focus on the mid-high frequency domain. The main goal of this paper is to address noise optimisation issues in the mid-high frequency range.

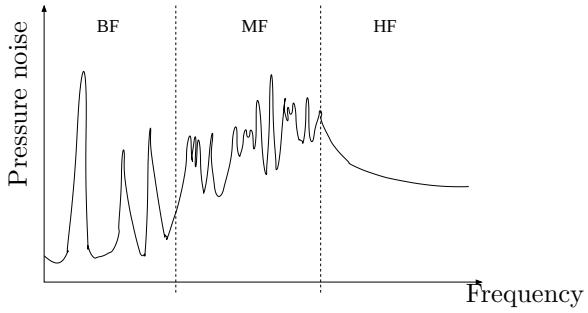

Figure 1: LF, MF and HF behaviours

The finite element method (FEM) is one of the most widely employed tools available for assessing the dynamic behaviour of such optimisation problems [1, 2]. Nevertheless, the excessive computational cost associated with solving large-size models, as required for example in the frequency response calculation, constitutes a major limitation with this method. Another limitation of the FEM is related to model reduction aspects when convergence of the "classical" reduced modal basis is not necessarily satisfied a priori in the short wavelength domain. More precisely, Silva et al. [1] proposed a method to maximise the absorption performance of insulating poroelastic systems using a coupled finite element model and evolutionary strategies. In reference [2], the main intention was to propose a numerical model of a room that allows computing the pressure field within the volume, in combination with a global optimisation algorithm. Analytical methods can also be used in the optimisation process for some situations. For instance, Dupont and Galland [13] applied analytical methods to optimise absorbing material locations in order to reduce the sound power transmitted by a plate. However, such an approach is limited to well defined and classical geometries.

Many authors have explored the topic of absorbing materials. Among them, let's cite M.A. Biot [15, 16], K. Attenborough [17] and J.F. Allard [18]. Our aim here is not to deal with such complex formulations, but instead to apply an energy method in order to optimise absorption coefficients on the boundaries of an acoustic cavity. In this context, a number of authors have already studied acoustical behaviour in damped cavities. Let's mention the work conducted for years in the area of prediction in cavities [20, 21, 22, 23, 24]. More recently, authors have been focusing on simplified models [19] and the optimisation of structures coupled with acoustic cavities [25, 26]. Energy methods are expected to offer many advantages. Such methods are well adapted to medium and high-

frequency situations and yield smaller matrices and fast optimisation processes. Moreover, energy methods are often used as alternatives in the high and medium frequency ranges. Among these methods, the most widespread remains the *Statistical Energy Analysis* (SEA) [3], which provides the mechanical energy of complex built structures. We have chosen to use a local energy formalism, as first proposed by Nefske and Sung [4] and improved by many subsequent authors [5, 6, 12, 8, 10, 28, 29, 30]. In the following discussion, this energy method will be called the Simplified Energy Method (or MES). MES has already been evaluated and validated for various elastic media such as beams [5, 7, 9], membranes and plates [5, 10], and acoustic cavities [7, 12]. This method has also been considered in both the transient and stationary cases [6, 7, 8].

The present paper is organised as follows. The first section will describe the optimisation problem. A definition of the inverse problem in terms of input-output data will then be presented. The input parameters for this optimisation process will also be recalled. The second section will summarise the Simplified Energy Method (MES) formulation. The direct MES problem will be raised in terms of calculating energy densities from both input power and dissipated power at the boundaries. The sensitivity of energy density to acoustic absorption will then be discussed. This study will show that a 200% change in the absorption coefficient α leads to only a 60% change in the pressure field inside the cavity: the results on α therefore will not be very robust. The intention here is for the outcome of these optimisation issues to yield an "on-off" response[1]. The lack of robustness in results is thus not considered to be that important. In order to improve time consumption statistics, a meta-model of energy distribution inside the cavity will be proposed. In this paper, the term "meta-model" refers to an analytical model of system behaviour. More specifically, it is a mathematical model along the lines of MES. This meta-model avoids the need to recalculate energy matrices during the optimisation loop. Lastly, a series of numerical experiments will be introduced and discussed. The optimisation routine proposed in this paper allows for fast calculations thanks to the reduced model size. Nevertheless, a number of limitations remain: the material is not being explicitly modelled; the porous medium is being modelled using an absorption coefficient; and damping inside the cavity has been ignored.

2 Simplified Energy Method (MES)

2.1 MES formulation

The Simplified Energy Method is based on a description of two local energy quantities. The first one is the total energy density W, defined as the sum of the potential energy density and the kinetic energy density. The second energy quantity I is the energy flow. The energy balance of such a system can be written as follows:

[1] "On" means that the absorption coefficient is set at its maximum value, while "off" means otherwise

$$\pi_{\text{diss}} = -\vec{\nabla} \cdot \vec{I} \tag{1}$$

where $\vec{\nabla}$ is the gradient operator. π_{diss} is the dissipated power density and may be neglected because the MES damping model, which is the same as SEA [3], can be written $\pi_{\text{diss}} = \eta\omega W$ with the damping loss factor $\eta << 1$ in acoustic fluids.

In this paper, we are particularly interested with the energy density W since it is proportional to the square pressure p^2 in the cavity, which is directly correlated with the sound level inside the cavity. Since W is a quadratic variable made of partial energy quantities corresponding to both direct and reverberated fields, the superposition principle can be applied:

$$W = W_{\text{dir}} + W_{\text{rev}} \tag{2}$$

In the following, an intrinsic energy law will be introduced (this law is often used to define the wave velocity c):

$$\vec{\mathbf{I}} = c \cdot \vec{W}.\vec{\mathbf{n}} \tag{3}$$

where $\vec{\mathbf{n}}$ is the normal outgoing unit vector. Equation 3 offers a basic definition of energy velocity; it clearly states that both energy flow and energy density serve to define energy velocity. This expression is well known and has already been demonstrated for general elastic media. A proof is available for instance in [14]. As an intrinsic law, this expression is adapted to all kinds of waves under eventual consideration.

The MES formulation is derived by considering a 3D space. Let's assume a symmetrical wave field along with Equations 3 and 1; the MES approach [12] leads to the following relation:

$$\frac{1}{r^2}\frac{\partial}{\partial r}\left(r^2\vec{I}\right) = 0 \tag{4}$$

which can also be written using equation 3, i.e.:

$$-c\frac{1}{r^2}\frac{\partial}{\partial r}\left(r^2 W\vec{\mathbf{n}}\right) = \vec{0} \tag{5}$$

Equation 4 stems directly from the energy balance, which is expressed in Equation 1. For unloaded lossless media (in this case, the acoustic domain) in the steady-state regime, Equation 1 under axisymmetric conditions simply leads to Equation 4.

The solution to Equation 5 corresponds to the radiosity method first proposed by Kuttruff [11].

A representation of both direct and reverberated fields is given in Figure 2.

The elementary solution of energy density is denoted G:

$$G(r) = \frac{1}{\gamma_0\, c}\,\frac{1}{r^2} \tag{6}$$

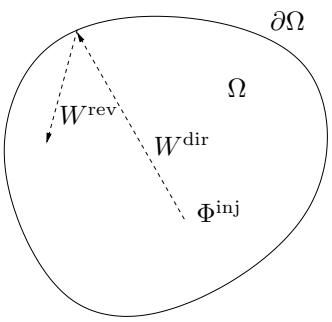

Figure 2: MES formulation: direct and reverberated fields

where γ_0 is the solid angle. The energy density inside the cavity can then be expressed as a function of the primary sources and fictitious sources located on the boundaries:

$$W(P) = \int_{\partial\Omega} \Phi(M)\vec{u}_{PM}.\vec{n}(M)G(M)\, d\partial\Omega + \int_{\partial\Omega} \sigma(M)\vec{u}_{PM}.\vec{n}(M)G(M)d\partial\Omega \quad (7)$$

where M is the integration point, $\vec{u}_{PM} = \frac{\overrightarrow{PM}}{\|\overrightarrow{PM}\|}$ and $\vec{n}(M)$ is the unit normal vector on $\partial\Omega$ at point M. $\Phi(P_0)$ is the acoustic boundary source and $\sigma(M)$ are fictitious boundary sources. We will use the term "boundary source" to denote those sources located on the cavity boundary (which may be due, for example, to external excitations).

The power balance on a point situated on a boundary allows expressing $\sigma(P)$ as follows:

$$\sigma(P) = [1-\alpha(P)]\left\{\int_{\partial\Omega, M\neq P} \sigma(M)\vec{u}_{PM}.\vec{n}G(M)d\partial\Omega + \int_{\Omega} \Phi(M)G(M)d\Omega\right\} \quad (8)$$

where $\alpha(P)$ is the absorption coefficient at point P. By discretizing Equation 8, σ can be expressed as a function of Φ.

2.2 Application

In this paper, MES is being applied through a matrix formulation. The equations from Section 2.1 are expressed as follows:

$$\vec{\sigma} = ([Id] - [\alpha])\,[T]\vec{\sigma} + ([Id] - [\alpha])\,[Q]\vec{\Phi} \tag{9}$$

where $[Id]$ is the identity matrix and $[\alpha]$ the diagonal matrix of the absorption coefficients. $[T]$ and $[Q]$ are matrices corresponding to the discretization of the integral formulations of Equation 8. Let's note that mesh size does not need to be fine for energy methods like MES, which only involve quadratic variables. The meshing criteria used in FEM or BEM would thus not be useful herein. A coarse mesh size is sufficient and allows for a rapid optimisation process. Equation 9 directly leads to $\vec{\sigma}$, as shown below:

$$\vec{\sigma} = ([Id] - [T] + [\alpha][T])^{-1}\,([Id] - [\alpha])\,[Q].\vec{\Phi} \tag{10}$$

W can then be expressed by discretizing equation 7, i.e.:

$$\vec{W} = [R]\vec{\Phi} + [S]\vec{\sigma} \tag{11}$$

Using equation 10, W can be rewritten as follows:

$$\vec{W} = \underbrace{\left([R] + ([Id] - [T] + [S][\alpha][T])^{-1}\,([Id] - [\alpha])\,[Q]\right)}_{[M(\alpha)]\ (n \times m \text{ matrix})}\vec{\Phi} \tag{12}$$

It is now possible to express the objective function $F(\vec{\alpha})$:

$$F(\alpha) = \sqrt{\left|\vec{\Phi}^T [M(\alpha)]^T [M(\alpha)]\vec{\Phi}\right|} \tag{13}$$

3 Optimisation problem

Let's consider the 3D acoustic cavity shown in Figure 3. Acoustic sources may be applied on the boundaries. Point sources inside the cavity will not be examined since the context of this paper is tied to the aircraft and automotive industries. Although the work programme outlined herein is quite academic and not directly related to industry, only those excitations caused externally will receive our attention. Such structures have already been studied by the authors in [27] and comparisons have been drawn between the MES method and both BEM and FEM methods, including a hybrid HMES method. The cavity structure has been discretised; for each boundary element, an absorption coefficient (which may depend on frequency) has been assigned. Once again, the aim of this paper is to optimise the distribution of absorption on elements in order to control acoustic energy within the acoustic domain.

The Simplified Energy Method (MES) has been described in depth in Section 2.1 above, and its implementation leads to a matrix formulation of the problem that can be written as follows:

$$\vec{W}\,(\alpha) = [M\,(\alpha)]\vec{\Phi} \tag{14}$$

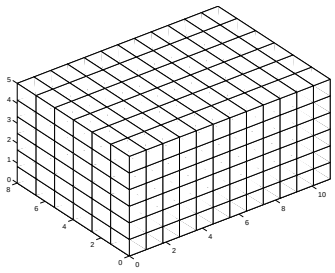

Figure 3: The acoustic finite element domain

Construction of the $n \times m$ matrix $[M(\alpha)]$ has been explained in Section 2.1. n represents the number of points where $\vec{W}$ will be calculated, while m is the number of facets originating from the discretisation of the structure. $\vec{W} = \{W_1,\ W_2,\ \ldots, W_n\}^T$ is the energy density vector inside the cavity, correlated with the square pressure. This vector is computed at n points, which will be referred to as *test points* in the following discussion. $\vec{\Phi} = \{\Phi_1,\ \Phi_2,\ \ldots, \Phi_m\}^T$ is the vector of input power on the boundaries, and $\vec{\alpha} = \{\alpha_1,\ \alpha_2,\ \ldots, \alpha_m\}^T$ is the vector of absorption coefficients on the boundaries. W can thus be computed for n points inside the cavity. Let's now define the quantity F to be minimised:

$$F(\vec{\alpha}) = \left\|\vec{W}\right\| = \sqrt{\sum_{i=1}^{n} W_i^2} \tag{15}$$

Function F is computed for a single frequency; a frequency averaging technique may be employed for instance whenever a more realistic definition of the impedance condition is introduced. Note that this function F is in fact identical to the L-2 norm of vector $\vec{W}$. Optimisation of noise level within the cavity can then be performed as follows:

- choosing n points in the cavity where the sound level is to be minimised;
- discretising the structure and computing the matrix $[M(\alpha)]$;
- applying an optimisation algorithm to minimise objective function F, with α_i $(1 < i < m)$ being the variables.

The goal of this paper is not to develop new optimisation algorithms, hence classical routines will be employed. In the next sections, we will develop the MES principle and its application to optimisation problems.

4 Results

4.1 Effects of α on W

The aim of this section is to analyse the influence of α on the W field in the cavity. Figure 4 shows the variation in W as a function of the variation in α.

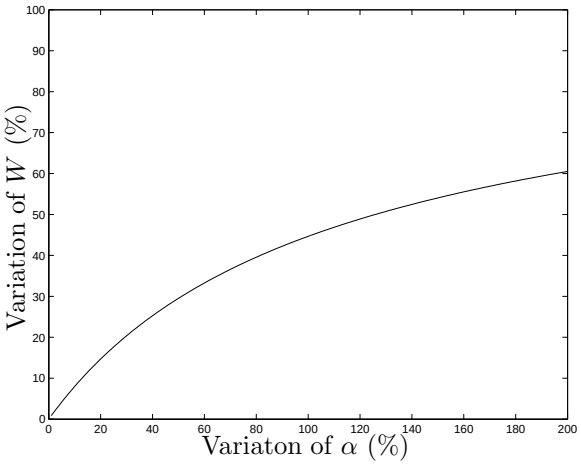

Figure 4: Variation in W vs. variation in α

Figure 4 indicates that large variations in α lead to minor variations relative to W. For example, a 100% variation in α leads to a 40% change in W, which therefore makes it impossible to obtain accurate results on the post-optimisation values of α. Nevertheless, optimisation can allow identifying positions where α should be increased.

4.2 Optimisation of α distribution

In this section, the position of absorbing materials will be optimised. The data used for this optimisation algorithm are given below in Table 1. It should be noted that these optimisation steps are performed at a single test point; consequently, results will depend on this particular point and should differ if the noise needs to be reduced at another point.

It is also important to notice that absorption coefficients for absorbing materials are always frequency-dependent. In this paper, we have not considered the frequency dependency aspect, but it could be included without any difficulty by solving the problem for each frequency or frequency band in the considered domain. Moreover, the results of this optimisation algorithm will demonstrate that the optimal value for is either 0 or 1. Including frequency-dependent coefficients would therefore yield the same results. Nevertheless, the energy method considered in this paper is only valid in the context of mid-high frequency prob-

lems. The optimisation problem is thus to be solved in a frequency range where modal overlap is quite high.

n	1
m	360
$\alpha_{\min}$	0
$\alpha_{\max}$	0.6
$\overline{\alpha}$ (mean)	0.3
First step	$\alpha = 0.3$
Box dimensions	$4 \times 2 \times 2$ m
Position of the source	$(2.83, 1.17, 0)$
Position of test point	$(1.33, 0.6, 0.6)$

Table 1: Input data used for optimisation routine

The optimisation algorithm is performed using a local gradient method. The aim of this paper has not been to develop new optimisation methods; consequently, an optimisation protocol subject to constraints has been adopted using the FMINCON function of the MATLAB software. This optimisation problem can then be formulated as follows:

$$\text{Minimising } F(\vec{\alpha}) = \sqrt{\left|\vec{\Phi}^T [M(\alpha)]^T [M(\alpha)] \vec{\Phi}\right|} \text{ so that } \begin{cases} 0 < \alpha < 1 \\ \sum_{i=1}^{N_\alpha} \dfrac{\alpha_i}{N_\alpha} = 0.3 \end{cases} \tag{16}$$

where N_α is the number of absorbing patches. Let's recall that every patch covers an equal area so that the mean value of α over these two quantities is the same. Keep in mind that the constraints on α prevent obtaining a trivial result (i.e. $\alpha = 1$ on all boundaries). In fact, these constraints are equivalent to setting the number of absorbing patches.

The result of this optimisation algorithm is given in Figures 5 and 6. Let's recall that the source is located at $(1.33, 0.6, 0.6)$, hence on the side not shown in the figures.

It is apparent that this algorithm leads to values of α equalto $\alpha_{\min}$ or $\alpha_{\max}$. The optimisation method is thus efficient for the purpose of optimising the position of absorbing materials, yet does not prove useful in determining the exact values of α. Regardless, we have shown in Section 4.1 that this kind of optimisation would not have been sufficiently robust.

The algorithm used in this optimisation problem is a local gradient algorithm, meaning that it requires initial values for α (see Table 1). Results depend on these initial values: the solution we derived may be a local solution and moreover it may be possible to obtain other solutions if other initial values were to be considered. For this reason, the next section will examine method robustness.

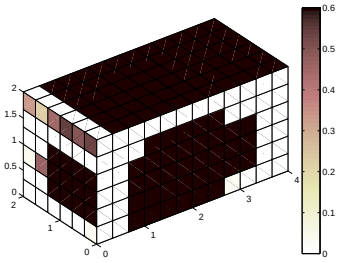

Figure 5: Optimisation result: distribution of α on the boundaries (top view) – white: $\alpha = 0$, black: $\alpha = 0.6$

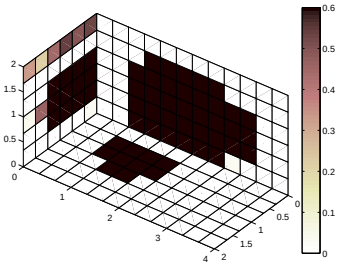

Figure 6: Optimisation result: distribution of α on the boundaries (bottom view) – white: $\alpha = 0$, black: $\alpha = 0.6$

4.3 Method robustness

In order to study the robustness of this method, several calculations have been carried out by considering various initial values.

From Figure 7, it can be observed that the final positions of absorbing materials remain independent of the initial values assigned to α. Moreover, certain initial values lie outside the range $0 < \alpha < 0.6$ and lead to similar results, which demonstrates method robustness. In conclusion, the method proves to be quite robust and suitable for use with any initial condition, α_{init}. Moreover, Figure 8 shows that noise level in the cavity after optimisation does not depend on init (at least for the case treated herein). Note that in Figure 8 the level of noise reduction can be defined as follows:

$$N_r = \frac{W_{\text{init}}}{W_{optim}} \times 100 \tag{17}$$

A good distribution of absorbing patches can thus serve to significantly reduce noise inside the cavity (at least at the considered test point).

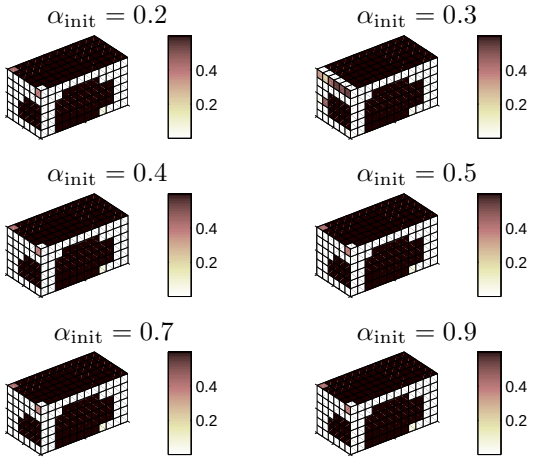

Figure 7: Study of method robustness

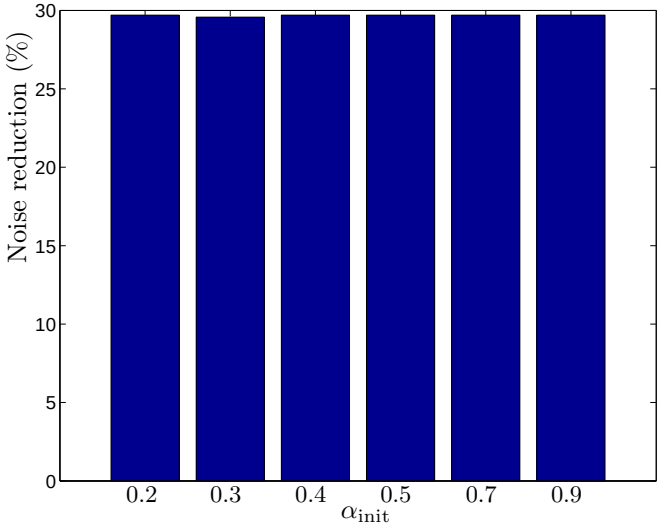

Figure 8: Noise reduction in the cavity N_r

A number of calculations have also been performed by considering two test points and several initial values (see Table 2). Results are shown in Figure 9: these results are also independent of the initial values of α.

Notice that the MES calculation protocol assumes lambertian directivity (ie.

1^{st} point	2^{nd} point
$x = 2.3$	$x = 1.2$
$y = 1.5$	$y = 1.5$
$z = 1.2$	$z = 1.2$

Table 2: Coordinates of the 2 test points used in these calculations

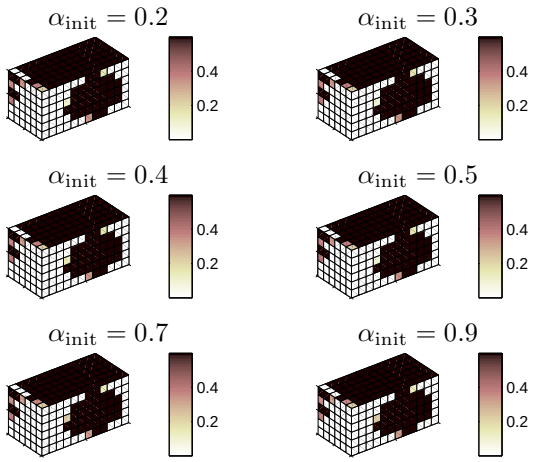

Figure 9: Method robustness: 2 test points

$d(\theta) = \frac{\cos\theta}{\pi}$). These results may differ when considering an alternative directivity. We have sought to use a uniform directivity $d(\theta) = \frac{1}{4\pi}$. Figure 10 displays the pertinent results; this figure has been obtained from a single test point and should be compared to results presented in Figure 7, which are significantly different. It would appear that knowing the directivity of the source is quite important.

5 Introduction of the meta-model for fast optimization

This section presents a meta-model designed for the absorption optimisation problem. Two reasons offer motivation for using meta-modelling techniques. The first relates to the type of predicted fields. The MES formulation normally predicts smooth energy behaviour, which can be very effectively represented through polynomial interpolation. MES also contains a number of drawbacks, including the high computational cost of energy resulting from the kinds of ma-

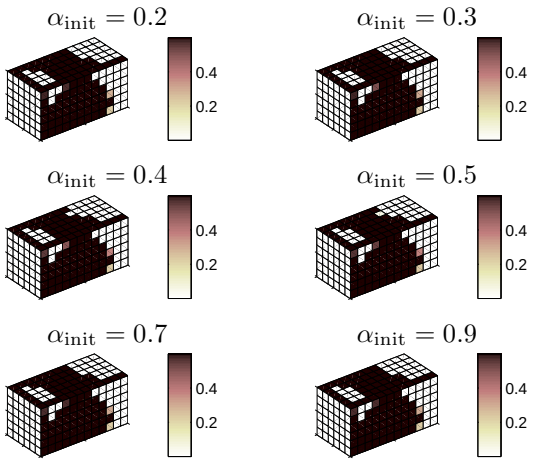

Figure 10: Method robustness: Uniform directivity

trices employed. The idea being introduced herein is a novel one compared to the authors' previous output. Moreover, calculations using the gradient method are costly because the gradients have to be calculated using discretisation methods. For these reasons, a meta-model has been proposed in this paper.

Since the problem solution is quite robust, we also suggest performing a polynomial interpolation in order to quickly derive the solution to the problem.

In considering Equation 14 applied to a single test point, it becomes possible to write the matrices and vectors corresponding to the problem solution as follows:

$$\vec{W}_{\text{sol}} = \vec{W}(\alpha_{\text{sol}}) = [M(\alpha_{\text{sol}})]\vec{\Phi} \tag{18}$$

$\vec{\alpha}_{\text{sol}}$ denotes the vector corresponding to the optimal solution of this problem. The dimension of $\vec{\alpha}_{\text{sol}}$ is thus equal to m, i.e. equal to the number of facets stemming from discretisation of the structure. In this section, we have rewritten Equation 18 as follows:

$$\vec{\alpha}(x, y, z) = [Z(x, y, z)]\vec{\xi} \tag{19}$$

where $\vec{\xi} = \left\{x, y, z, x^2, y^2, z^2, xy, xz, yz\right\}^T$ and the dimension of matrix $\vec{Z}$ is (n, N), with N dependent on the degree of polynomial interpolation ($N = 10$ in the present case).

Matrix $\vec{Z}$ can then be built by:

- performing p optimisation algorithms $\rightarrow \left\{[\alpha^1_{\text{sol}}], [\alpha^2_{\text{sol}}], \ldots, [\alpha^p_{\text{sol}}]\right\}$;

1^{st} point	2^{nd} point	3^{rd} point	4^{th} point
$x = 2.3$	$x = 1.3$	$x = 3.1$	$x = 0.7$
$y = 1.5$	$y = 0.5$	$y = 1.2$	$y = 1.2$
$z = 1.2$	$z = 1.7$	$z = 1.4$	$z = 0.4$

Table 3: Coordinates of the 4 test points used in these calculations

- linking these solutions to the test point positions: $\vec{\alpha}^j_{\text{sol}} = \vec{Z}^j\vec{\xi}^j$, where $\vec{\xi}^j = \left\{x^j, y^j, z^j, (x^j)^2, (y^j)^2, (z^j)^2, x^jy^j, x^jz^j, y^jz^j\right\}^T$, $j \in [1, p]$ and the dimension of matrix $\vec{Z}^j$ equals (n, N);
- interpolating the system in order to be able to consider any test point;
- changing the values obtained of α in order to satisfy the constraints ($0 \leq \alpha \leq 0.6$). The results reported in section 4.2 indicate that the values of α were either $\alpha = 0$ or $\alpha = 0.6$, which leads us to apply the following changes to the results:
  - $\alpha < 0.3 \Rightarrow \alpha = 0$
  - $\alpha > 0.3 \Rightarrow \alpha = 0.6$

The results of this optimisation method are illustrated in Figure 11. The noise level has been set equal to 1 in the case of a non-optimised configuration ($\alpha = 0.3$ everywhere on the boundaries). These calculations were performed for 4 different test points, which have been summarised in Table 3.

Figure 11 shows that the polynomial interpolation approach is not as efficient as full optimisation; nevertheless, it provides for good results at a very low calculation cost. Moreover, these results yield an initial result that is applicable to the initial values for full optimisation. Other polynomial interpolations have been conducted by considering 4th and 6th-order interpolations. Results are given in Figures 12 and 13. Since these results show no improvement, the second order proves to be sufficient (in the special case of a box-like cavity, as studied in this work). The reason why orders above 2 do not improve results should be related to the fact that approximations are inappropriate due to the 0-1 nature of absorption coefficient values. Moreover, the exact form of the solution should not match any of the higher polynomial forms, and the "right" solution seems to be quite regular (i.e. the solution should be an approximation when considering a simple function).

6 Conclusion

In this paper, we have demonstrated the efficiency of optimising the position of absorbing materials on boundaries of a cavity. Results prove to be satisfactory even though the optimisation algorithm requires initial values; these results do not depend on initial values in the special case of the box-like cavity studied

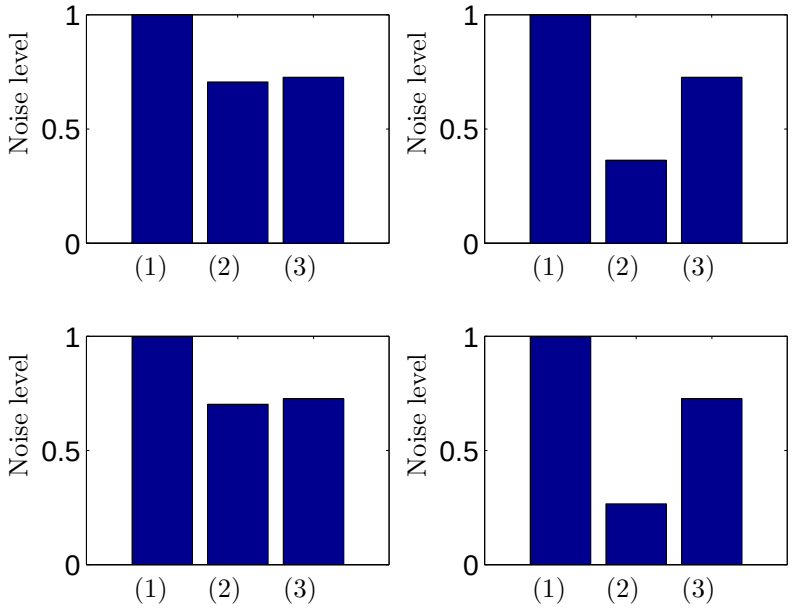

Figure 11: Noise reduction: comparison between full optimisation and polynomial interpolation: (1) initial values, (2) full optimisation, (3) fast optimisation

herein. It has been found however that optimisation results do depend on the source directivity, which must be evaluated before conducting the MES calculations. In order to perform a rapid optimisation, we have also proposed a polynomial interpolation, obtained using just 8 calculation points; these calculations have been run using only 8 fully-optimised points. Results fall short of the full optimisation results, yet the method allows reducing noise level in the cavity.

References

[1] Silva, F. and Pavanello, R., An Evolutionary Optimization Method applied to Absorbing Poroelastic Systems, Acoustical Society of America Journal, vol. 123, pp. 3571 (2008)

[2] Dutilleux, G., Sgard, F. C. and Kristiansen, U. R., Low-frequency assessment of the in situ acoustic absorption of materials in rooms: an inverse problem approach using evolutionary optimization, Int. J. Numer. Meth. Engng 2002; 53:21432161

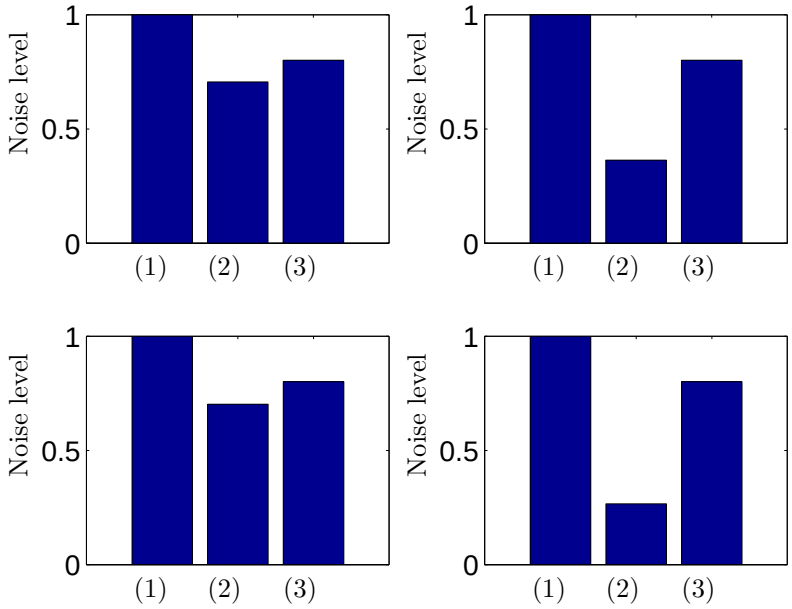

Figure 12: Noise reduction: comparison between full optimisation and 4^{th} degree polynomial interpolation: (1) initial values, (2) full optimisation, (3) fast optimisation

[3] R. H. Lyon, Statistical Energy Analysis of Dynamical Systems: Theory and Application, Cambridge, Massachusetts, MIT Press, 1975.

[4] D. Nefske, S. Sung, Power flow finite element analysis of dynamic systems: Basic theory and application to beams, NCA Publication 3.

[5] Y. Lase, M. Ichchou, L. Jezequel, Energy analysis of bars and beams: Theoretical formulations, Journal of Sound and Vibration 192 (1996) 281–305.

[6] F. Sui, M. Ichchou, L. Jezequel, Prediction of vibroacoustics energy using a discretized transient local energy approach and comparison with TSEA, Journal of Sound and Vibration 251 (2002) 163–180 .

[7] A. Wang, N. Vlahopoulos, K. Wu, Development of an energy boundary element formulation for computing high-frequency sound radiation from incoherent intensity boundary conditions, Journal of Sound and Vibration (2004), vol. 278, no1-2, pp. 413-436.

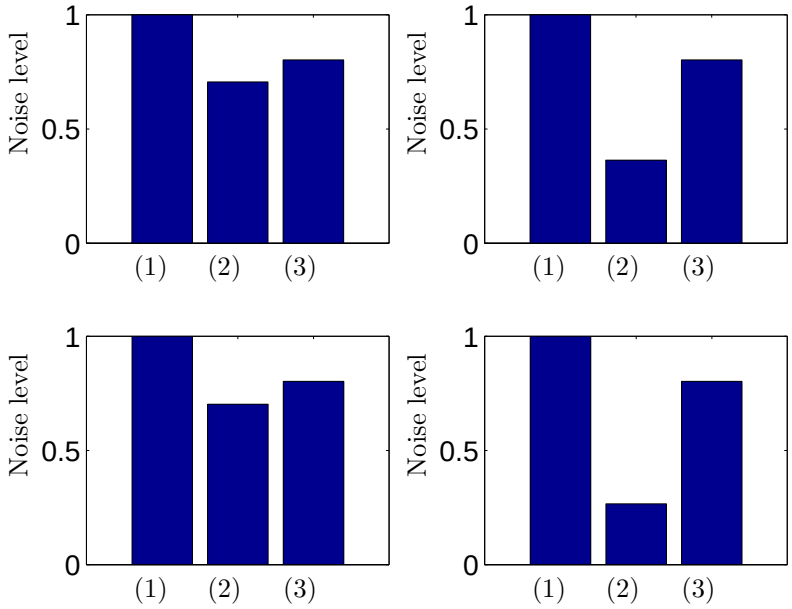

Figure 13: Noise reduction: comparison between full optimisation and 6^{th} degree polynomial interpolation: (1) initial values, (2) full optimisation, (3) fast optimisation

[8] M. Ichchou, A. Le Bot, L. Jezequel, A transient local energy approach as an alternative to transient SEA: wave and telegraph equations, Journal of Sound and Vibration 246 (2001) 829–840.

[9] M. Ichchou, S. Akrout, J. M. Mencik, Guided waves group and energy velocities via finite elements, Journal of Sound and Vibration 305 (2007) 931–944.

[10] P. Hardy, M. Ichchou, L. Jezequel, D. Trentin, A hybrid local energy formulation for plates mid-frequency flexural vibrations, European Journal of Mechanics - A/Solids, 28 (2009) 121-130.

[11] Kuttruff, H., 1997. Energetic sound propagation in rooms. Acoustica with Acta Acoustica 83, 622–628.

[12] Ichchou, M., Jezequel, L., 1996. Comments on simple models of the energy flow in vibrating membranes and transversely vibrating plates. Journal of Sound and Vibration 195, 679–685.

[13] Dupont, J-B. and Galland, M-A., Active absorption to reduce the noise transmitted out of an enclosure, Applied Acoustics, Volume 70, Issue 1, January 2009, Pages 142-152

[14] L. Brillouin, Tensors in mechanics and elasticity, Academic Press, 1964

[15] M.A. Biot, Theory of Propagation of Elastic Waves in a Fluid-Saturated Porous Solid. I. Low-Frequency Range, ASA, 1956, The Journal of the Acoustical Society of America, 28 (2), 168-178

[16] M.A. Biot, Theory of Propagation of Elastic Waves in a Fluid-Saturated Porous Solid. II. Higher-Frequency Range, 1956 Acoustical Society of America Journal, 28, 179-+

[17] K. Attenborough, Acoustical characteristics of rigid fibrous absorbents and granular media, J. Acoust. Soc. Am. 73 (1983) 785-799

[18] J. F. Allard, A. Aknine, and C. Depollier, Acoustic properties of partially reticulated foams with high and medium ow resistance, J. Acoust. Soc. Am., 79 (1986) 1734-1740

[19] S. Besset and L. Jézéquel, Optimization of characteristics of porous materials based on a modal synthesis method, European Journal of Mechanics - A/Solids, 28 (1), 102-109, 2009

[20] E.H. Dowell, G.F. Gorman III and D.A. Smith, Acoustoelasticity: General theory, acoustic natural modes and forced response to sinusoidal excitation, including comparisons with experiment, Journal of Sound and Vibration, 52(4), 519-542, 1977

[21] A. Trochidis and A. Kalaroutis, Sound transmission through double partitions with cavity absorption, Journal of Sound and Vibration, 107(2), 321-327, 1986

[22] S. Suzuki and S. Maruyama and H. Ido, Boundary element analysis of cavity noise problems with complicated boundary conditions, Journal of Sound and Vibration, 130(1), 79–96, 1989

[23] Kimihiro Sakagami and Masakazu Kiyama and Masayuki Morimoto and Daiji Takahashi, Sound absorption of a cavity-backed membrane: A step towards design method for membrane-type absorbers, Applied Acoustics, 49(3), 237–247, 1996

[24] A. Craggs, Coupling of finite element acoustic absorption models, Journal of Sound and Vibration, 66(4), 605-613, 1979

[25] T. Yamamoto and S. Maruyama and S. Nishiwaki and M. Yoshimura, Thickness optimization of a multilayered structure on the coupling surface between a structure and an acoustic cavity, Journal of Sound and Vibration, 318(1-2), 109-130, 2008

[26] T. Yamamoto and S. Maruyama and S. Nishiwaki and M. Yoshimura, Topology design of multi-material soundproof structures including poroelastic media to minimize sound pressure levels, Computer methods in applied mechanics and engineering, 198(17-20), 1439–1455, 2009

[27] S. Besset, M.N. Ichchou and L. Jzquel, A coupled BEM and energy flow method for mid-high frequency internal acoustic, Journal of Computational Acoustic, Vol. 18, No. 1 (2010) 6985.

[28] M. N. Ichchou, A. Le Bot and L. Jézéquel, A transient local energy approach as an alternative to transient sea: Wave and telegraph equations, Journal of Sound and Vibration, Volume 246, Issue 5, 4 October 2001, Pages 829-840.

[29] FS Sui,MN Ichchou, L. Jézéquel, Prediction of vibroacoustics energy using a discretized transient local energy approach and comparison with TSEA, Journal of Sound and Vibration, Volume 251, Issue 1, 14 March 2002, Pages 163-180.

[30] F. Sui and M. N. Ichchou, Prediction of Time-Varying Vibroacoustic Energy Using a New Energy Approach, J. Vib. Acoust. 126, 184 (2004).